# Channel Estimation and Prediction for Adaptive OFDM Downlinks

Mikael Sternad and Daniel Aronsson
Signals and Systems, Uppsala University, PO Box 528,SE-751 20 Uppsala, Sweden
{daniel.aronsson,mikael.sternad}@signal.uu.se, tel. +46 18 4713078, fax +46 18 555096

***Abstract*— Channel estimation and prediction algorithms are developed and evaluated for use in broadband adaptive OFDM downlinks over fading channels for vehicular users. Accurate channel estimation may be obtained by using a combined pilot-aided and decision-directed approach based on Kalman filtering and prediction. The correlation properties of the channel in both time and space are taken into account. Kalman performance at much lower computational complexity is attained with recently developed constant gain adaptation laws. We present and evaluate a state-space realization of such an adaptation law, with computational complexity of the order of the square of the number of parallel tracked pilot subcarriers. In an adaptive OFDM system, prediction of the channel power a few milliseconds ahead will also be required. Frequency-domain channel estimates can be transformed to the time domain, and used as regressors in channel predictors based on linear regression. We also make a preliminary evaluation of the direct use of complex channel prediction in the frequency domain for channel power prediction.**

## I. Outline

Adaptive transmission can radically improve the spectral efficiency when multiple users have independently fading links. The users may then share the available bandwidth, and resources are allocated to terminals who need them best and/or can utilize them best via link adaptation. This paper focuses on the downlink of an adaptive OFDM system that employs Frequency Division Duplex (FDD).[1] The aim is to attain high spectral efficiency for wide area coverage and to serve also vehicular users, with velocities around 100 km/h.

In this adaptive OFDM downlink, packet data streams to a number of active users are multiplexed on a common bandwidth. Each user must estimate and predict the channel over the whole utilized bandwidth, and report which parts of the spectrum will have the best signal to interference ratio. A scheduler, located at the base station, then allocates time-frequency resources based on the requirements and channel qualities of each user. This system is outlined in Section II and is discussed in more detail in [2] and [3].

Channel estimators located in terminals of such systems would have to meet three challenges:

1) The OFDM channel must be estimated with sufficient accuracy so that payload information can be detected also when using high modulation formats. Otherwise, a high spectral efficiency becomes unattainable.
2) The fading channel must be predicted with sufficient accuracy over time horizons that correspond to the feedback delay of the adaptive transmission system.
3) The computational complexity of the estimator must be limited, both to reduce the computational delays and to attain low power consumption at terminals.

The present paper outlines research aimed at meeting the above requirements. We start from a combined pilot-aided and decision directed channel estimator in the form of a Kalman state estimator. This estimator is based on ARMA models of the fading and on frequency domain covariance information. It provides minimal mean square estimation errors (MMSE estimates) at the pilot locations. The main computational complexity of this Kalman algorithm resides in the required update of a Riccati difference equation. That update may be avoided by using the recently developed General Constant Gain (GCG) class of adaptation laws [4], which are well suited to the present problem. They provide performance close to that of the Kalman algorithm, but with much lower computational complexity. In this paper, we present and evaluate a GCG algorithm in state-space form.

The performance of the algorithms is evaluated on flat Rayleigh fading simulated channels. We also present preliminary results for measured channels, obtained from channel sounding in an suburban environment.

## II. The Proposed Adaptive OFDM Downlink

We assume the use of FDD, and of a base station infrastructure with sectored antennas. User terminals are in this paper assumed to have only one antenna.

The available downlink bandwidth within a sector (cell) is assumed to be slotted in time. Each slot of duration $T$ is furthermore partitioned into *time-frequency bins* of bandwidth $\Delta f_b$. We here assume $T = 0.667$ ms and $\Delta f_b = 200$ kHz, which is appropriate for stationary and vehicular users in urban or suburban environments [3]. We also assume a subcarrier spacing of 10 kHz, a cyclical prefix of length $11\mu$s and an OFDM symbol period (including cyclic prefix) of $T_s = 111\mu$s. Thus, each bin of 0.667 ms $\times$ 200 kHz carries 120 symbols, with 6 symbols of length $111\mu$s on each of the 20 10 kHz subcarriers. Of these 120 symbols, 12 are allocated for training and downlink control, leaving 108 payload symbols, see Fig. 1.

During slot $j$, each terminal predicts the signal to interference and noise ratio (SINR) for all bins, with a prediction horizon $mT$ that is larger than the time delay of the transmission control loop. All terminals then signal their predicted quality estimates on an uplink control channel. They transmit the suggested appropriate modulation formats to be used within all bins of the predicted time slot $j+m$. A scheduler that is located at the base station then allocates these time-frequency bins exclusively to different users and broadcasts its allocation

[1]The system serves as a focus for research within the Wireless IP project [1], supported by the Swedish Foundation for Strategic Research SSF.

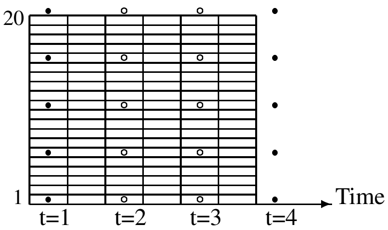


Fig. 1. One of the time-frequency bins of the proposed system, containing 20 subcarriers with 6 symbols each. Known 4-QAM pilot symbols (black) and 4-QAM downlink control symbols (rings) are placed on four pilot subcarriers. The modulation format for the other (payload) symbols is adjusted adaptively. All payload symbols within a bin use the same modulation format.

decisions by using some of the downlink control symbols. In the subsequent downlink transmission of slot $j+m$, the different modulation formats used in different bins are those which were suggested by the appointed users.

For the payload symbols, we utilize an adaptive modulation system that uses 8 uncoded modulation formats: BPSK, 4-QAM, 8-QAM, 16-QAM, 32-QAM 64-QAM, 128-QAM, and 256-QAM, with constant transmit power [3]. The use of 256-QAM requires SNR $\geq$ 30 dB, and a correspondingly low channel estimation error.

The 12 pilots and control symbols are located within each bin as indicated by Fig. 1. They are assumed to use 4-QAM and can be detected by all users within the sector. (The sector boundary is defined as the range at which 4-QAM symbols can on average be detected with low probability of error.)

The spacing between pilots in time, 0.666 ms, corresponds to 0.115 wavelengths at 1.9 GHz carrier frequency and 100 km/h vehicle speed. Pilot symbols are transmitted over every fifth subcarrier, in the following denoted *pilot subcarriers*. Their spacing in frequency, 50 kHz, is designed to be adequate to handle the frequency selectivity encountered in suburban propagation environments.

Thus, all active users must estimate the channel within the whole bandwidth. The channel estimates are used for two purposes: In bins addressed to a user, the payload symbols are de-rotated for coherent detection. Channel estimates for all bins are furthermore used by the predictor.

## III. Channel estimation

The received scalar complex-valued baseband signal $y_{n,t}$ on the pilot subcarrier $n$ is described by

$$y_{n,t} = s_{n,t} h_{n,t} + v_{n,t} \quad , \tag{1}$$

where the time index $t$ will here be incremented in steps of two symbol times $2T_s = 222\mu$s, $s_{n,t}$ is a pilot or control symbol, $h_{n,t}$ is the scalar complex channel and $v_{n,t}$ represents noise and interference, with zero mean and variance $\sigma_v^2$.

Pilot-based channel estimates could be obtained at all locations where $s_{n,t}$ are known 4-QAM pilot symbols as

$$\hat{h}^p_{n,t} = y_{n,t} s^*_{n,t} = h_{n,t} + v_{n,t} s^*_{n,t} \quad , \tag{2}$$

since $s_{n,t} s^*_{n,t} = 1$. In a second step, the noise $v_{n,t} s^*_{n,t}$ can be reduced by 1-D or 2-D MMSE (Wiener) filtering, see e.g. [5], [6], [7]. The downlink control symbols can furthermore be utilized in a decision-directed scheme. (However, note that the payload symbols of all bins cannot be used for decision-directed channel estimation. They may be destined for other users and may therefore use high modulation formats that cannot be detected reliably by the terminal of interest.)

2-D FIR Wiener filtering of a set of $p$ subcarriers at time $t$, using a block of $pN$ estimates given by (2) at $p$ different frequencies from $N$ time instants $\tau = t, \ldots, t-N$, would require on the order of $p^2 N$ complex operations. Our aim will be to obtain an algorithm that corresponds to a 2-D IIR Wiener filter, with infinite support backward in time. It should require only $p^2 c$ operations, where $c$ is small, for the same calculation. The derivation of such an algorithm begins with the Kalman estimator for linear regressions of the form (1).

## IV. Kalman Channel Estimation

Our aim is to simultaneously estimate a set of $p$ channel coefficients $h_{n,t}, n = 1, \ldots, p$ recursively in time, based on $p$ measurements $y_{n,t}, n = 1, \ldots, p$.

The scalar complex channel coefficients $h_{n,t}$ are described by ARMA models of order $n_D$ in state space form,

$$x_{n,t+1} = \mathbf{F} x_{n,t} + \mathbf{G} e_{n,t} \quad ; \quad h_{n,t} = \mathbf{H} x_{n,t} \ , \tag{3}$$

with scalar driving noises $e_{n,t}$. The same ARMA model will be used to describe the fading statistics on all pilot subcarriers. To utilize the frequency-domain correlation of $h_{n,t}$ in the estimation, one should use a model with combined state vector

$$x_t = (\ x^T_{1,t} \ldots x^T_{p,t})^T \tag{4}$$

of length $n_x = p n_D$, that simultaneously describes the $p$ measurements and the $p$ channel coefficients

$$y_t = (\ y_{1,t} \ldots y_{p,t}\ )^T \quad ; \quad h_t = (\ h_{1,t} \ldots h_{p,t}\ )^T \quad . \tag{5}$$

Such a model is given by

$$\begin{aligned} x_{t+1} &= \text{diag}(\mathbf{F}) x_t + \text{diag}(\mathbf{G}) \text{diag}(e_{n,t}) \quad = \mathbf{A} x_t + w_t \\ h_t &= \text{diag}(\mathbf{H}) x_t \\ y_t &= \text{diag}(s_{n,t}) \text{diag}(\mathbf{H}) x_t + \text{diag}(v_{n,t}) = \mathbf{C}_t x_t + v_t \ . \end{aligned} \tag{6}$$

Here, diag$(\cdot)$ represents (block)diagonal matrices. The ARMA model of $h_{n,t}$ describes the correlation in time (or Doppler spectrum). The covariance matrix $\mathbf{R}_v$ of $v_t = \text{diag}(v_{n,t})$ describes the frequency-domain correlation of the noise and interference, while the covariance matrix $\mathbf{R}_w$ of $w_t = \text{diag}(\mathbf{G})\text{diag}(e_{n,t})$ describes the frequency-domain correlation of the channel taps $h_{n,t}$. These parameters can be adjusted to the data series, either periodically or recursively. If this is impractical, simple and robust choices can be used. Robust selections are suggested by [6].

The Kalman filter estimate $\hat{h}_{t|t}$, and the predictor estimate $\hat{h}_{t+L|t}$, are then given by [8], [9]

$$\begin{aligned} \varepsilon_t &= y_t - \mathbf{C}_t \hat{x}_{t|t-1} && (7)\\ \hat{x}_{t|t} &= \mathbf{A}\hat{x}_{t-1|t-1} + \mathbf{K}_t^f \varepsilon_t && (8)\\ \hat{x}_{t+1|t} &= \mathbf{A}\hat{x}_{t|t} && (9)\\ \hat{h}_{t|t} &= \mathrm{diag}(\mathbf{H})\hat{x}_{t|t} && (10)\\ \hat{h}_{t+L|t} &= \mathrm{diag}(\mathbf{H})\mathbf{A}^L \hat{x}_{t|t} \quad . && (11) \end{aligned}$$

Note that the output matrix $\mathbf{C}_t = \mathrm{diag}(s_{n,t}\mathbf{H})$ of (6) is time-varying. Therefore, the Kalman filter gain matrix $\mathbf{K}_t^f$ will also be time-varying. It is updated by iterating a Riccati difference equation forward in time.

This algorithm can be applied in several ways on a set of $p$ pilot subcarriers. A decision-directed algorithm which produces estimates at $t = 1, 2, 3, \ldots$, proceeds as follows. At time $t = 1$, a Kalman estimator will use the received signal $y_1$, the known pilots $s_{n,1}, n = 1, \ldots, p$ and its previous state $\hat{x}_{0|0}$ to obtain a filtering estimate $\hat{h}_{1|1}$ of the channels at $t = 1$ and a one-step prediction $\hat{x}_{2|1}$ and $\hat{h}_{2|1}$ for $t = 2$. The $p$ downlink control symbols $s_{n,2}$ are then detected, using

$$\hat{s}_{n,2} = f(y_{n,2}/\hat{h}_{n,2|1}) \quad n = 1, \ldots, p \quad , \tag{12}$$

where $f(\cdot)$ is the decision nonlinearity. This procedure is repeated at $t = 2$ and $t = 3$. At $t = 4$, training symbols are available and estimation is performed as for $t = 1$.

## V. Channel Estimation by a Constant-Gain Kalman Approximation

A theory for designing constant-gain Wiener-LMS adaptation laws in transfer operator form was presented in [4], [10]. We here outline how this framework can also be used to approximate Kalman estimators by state observers with constant gains. Starting from (6), define the regressor covariance matrix

$$\mathbf{R} = \mathrm{E}\left[\mathrm{diag}(s_{n,t}^*)\mathrm{diag}(s_{n,t})\right] \quad , \tag{13}$$

the autocorrelation matrix noise, given by

$$\mathbf{Z}_t = \mathrm{diag}(s_{n,t}^*)\mathrm{diag}(s_{n,t}) - \mathbf{R} \quad , \tag{14}$$

the gradient noise, given by

$$\eta_t = \mathbf{Z}_t(h_t - \hat{h}_{t|t-1}) + \mathrm{diag}(s_{n,t}^*)v_t \quad , \tag{15}$$

and the alternative measurement signal $f_t$, of dimension $p$,

$$f_t = \mathbf{R}\hat{h}_{t|t-1} + \mathrm{diag}(s_{n,t}^*)\varepsilon_t = \mathbf{R}h_t + \eta_t \quad . \tag{16}$$

For the last equality, please see (14),(15) in [4]. Instead of the state space model (6), which has a time-varying output matrix $\mathbf{C}_t$, and thus requires a time-varying Kalman gain, we may now instead consider the linear time-invariant model

$$\begin{aligned} x_{t+1} &= \mathbf{A}x_t + w_t && (17)\\ f_t &= \mathbf{R}h_t + \eta_t = \mathbf{R}\,\mathrm{diag}(\mathbf{H})x_t + \eta_t && (18) \end{aligned}$$

where $\eta_t$ acts as measurement noise. The steady-state Kalman state estimator for the model (17),(18) constitutes the General Constant Gain *(GCG)* estimator for the original model (6). It is given by (7)-(11), but with (8) exchanged for

$$\hat{x}_{t|t} = \mathbf{A}\hat{x}_{t-1|t-1} + \mathbf{K}(f_t - \mathbf{R}\,\hat{h}_{t|t-1}) \quad . \tag{19}$$

The steady-state filter gain matrix $\mathbf{K}$ is calculated via an algebraic Riccati equation, which needs to be recalculated only when the model (17),(18) is changed. The covariance matrix of the gradient noise $\eta_t$ is required in that calculation. The feedback via the estimation error in (15) would here in general require the use of an iterative design, as suggested in [4]. However, in our case, where the symbols $s_{n,t}$ are 4-QAM and thus have constant modulus $s_{n,t}s_{n,t}^* = 1$,

$$\mathrm{diag}(s_{n,t}^*)\mathrm{diag}(s_{n,t}) = \mathbf{I} = \mathbf{R}$$

so $\mathbf{Z}_t = \mathbf{0}$. Thus, the gradient noise (15) is in this case

$$\eta_t = \mathrm{diag}(s_{n,t}^*)v_t \quad , \tag{20}$$

with covariance matrix $\mathbf{R}_\eta = \mathbf{R}_v$. The total number of complex multiplications required per time step will, with a state vector $x_t$ of length $n_x = pn_D$, be[2]

$$5n_x + pn_x = 5pn_D + p^2 n_D \quad . \tag{21}$$

The order $n_D$ of the ARMA fading model can in general be chosen small, $n_D \leq 4$, see [11].

## VI. Channel Interpolation within Bins

The channels may vary significantly within bins. For the purpose of coherent detection of payload symbols destined to "our" terminal, the channel estimates on pilot subcarriers must be interpolated over the payload symbols. We use 2D quadratic interpolation, a method also discussed in e.g. [12]. (Other methods, such as Wiener interpolation, could also be used.) A 2D quadratic interpolation of the complex channel within the bin is fitted to the estimated channels at $t = 1, 2, 3$ and $t = 4$ (early in the next bin), using also a pilot carrier outside the bin (subcarrier number 21 in Fig. 1). Payload symbols are then detected as $f(y_{i,j}/\bar{h}_{i,j})$, where $\bar{h}_{i,j}$ is the interpolated channel estimate at symbol location $i, j$ within the bin.

## VII. Channel Power Prediction

A long-term prediction of the channel power is required for allocating the resources and determining the modulation formats to be used in future bins. One alternative is to use the $L$-step prediction (11) to extrapolate the estimated complex channels on all pilot subcarriers $2L$ symbols into the future.

The square of the predicted complex tap would then constitute a biased prediction of the channel power [13]. If $h_{n,t}$ has zero mean, an unbiased quadratic prediction estimate of the power $p_{n,t+L}$ of pilot carrier $n$ is obtained as ([14] p. 162)

$$\hat{p}_{n,t+L|t} = |\hat{h}_{n,t+L|t}|^2 + \sigma_h^2 - \sigma_{\hat{h}}^2 \quad , \tag{22}$$

[2]If a complex-valued diagonal realization is used in (3), which is attractive numerically, then the number of complex multiplications required in (7), (9), (10) and (11) will all be (at most) $n_x$ each, while (19) requires $n_x + n_x p$ multiplications, since the dimension of $\mathbf{K}$ is $n_x$ by $p$.

where $\sigma_h^2$ and $\sigma_{\hat{h}}^2$ are the variances of $h_{n,t}$ and $\hat{h}_{t+L|t}$, respectively.

Alternatively, we may use the Kalman or GCG estimators as noise-reducing front-ends to the time-domain estimator that were presented and investigated in [13] and [14]. It is at present unclear which of these two strategies provides the best performance and this question is under current investigation.

An appropriate measure for evaluating power prediction algorithms is the normalized mean square power estimation error (NMSE)

$$\text{NMSE} = \frac{\text{E}\,||h_{n,t}|^2 - \hat{p}_{n,t|t-L}|^2}{\text{E}\,|h_{n,t}|^4} \quad . \tag{23}$$

## VIII. Evaluation on Flat Rayleigh Fading Channel

The methods outlined in Section IV-VII are now evaluated. We begin by applying the Kalman and the GCG channel estimators on a simulated flat Rayleigh fading 5 MHz channel at 1900 MHz. The terminal has velocity 100 km/h, so the maximal Doppler frequency $f_D$ is 174 Hz and $f_D T_s = 0.0193$. The noise $v_{n,t}$ is uncorrelated in time and among subcarriers. The 5 MHz bandwidth is partitioned into 25 bins. We begin by using 25 parallel estimators, which each uses $p = 4$ pilot subcarriers. Thus, one estimator is used for each bin width. We first investigate the Channel Signal-to-Error Ratio (SER) of the estimator output, defined by

$$\text{SER} = \frac{\text{E}\,|h_{n,t}|^2}{\text{E}\,|\tilde{h}_{n,t|t-L}|^2} \tag{24}$$

where $\tilde{h}_{n,t|t-L} = h_t - \hat{h}_{n,t|t-L}$. Both the Kalman and the GCG algorithms are based on autoregressive models of order 4 that are adjusted to the Jakes fading spectrum. Correct estimates of the noise and channel covariances are used. The resulting SER as a function of the SNR, shown in Fig. 2, is identical for the Kalman and the GCG algorithm. A significant noise reduction SER - SNR is observed. When estimated regressors are used at the downlink control locations, the performance degrades at low SNR's. An increase of the estimator width $p$ results in the expected noise averaging effect: Each doubling of $p$ results in a 3 dB SNR improvement of the SER performance curves.

We then investigate the performance of the 2-D quadratic channel interpolation. Kalman and GCG filter estimates on the pilot and control locations shown in Fig. 1 are interpolated as described in Section VI. Since the channel power is varying between bins, the local SNR will vary both between and within bins. The symbol error rate is approximately determined by the worst SNR (lowest channel power) within the bin [3]. We use this SNR measure, $\text{SNR}_{mb} = \min_{\text{bin}} |h_{n,t}|^2/\sigma_v^2$, and compare it to the bin-averaged SER, defined by

$$\text{SER}_b = \frac{\text{E}_{\text{bin}}|h_{n,t}|^2}{\text{E}_{\text{bin}}|\tilde{h}_{n,t}|^2} \quad . \tag{25}$$

As long as $\text{SER}_b > \text{SNR}_{mb}$, the bit error rate for detected payload symbols will essentially be determined by the noise level, rather than by the estimation error. According to Fig. 3, this will be the case for flat Rayleigh fading channels.

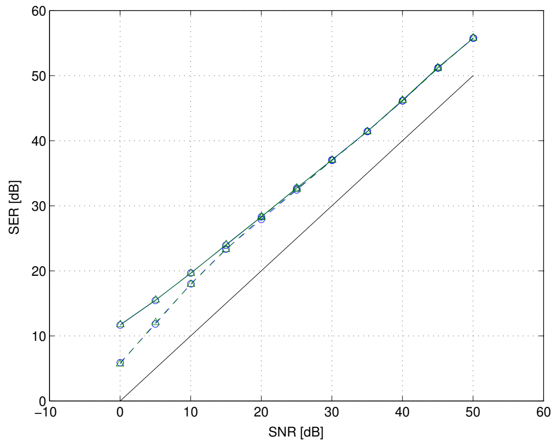


Fig. 2. Channel signal to estimation error ratio (SER) for a Jakes flat fading channel at 100 km/h, as a function of the SNR. Kalman (rings) and GCG (triangle) filter estimates $\hat{h}_{n,t|t}$ are obtained when using correct regressors (solid) and when using estimated downlink control symbols (12) (dashed). The curves overlap. The solid line SER=SNR is added for comparison.

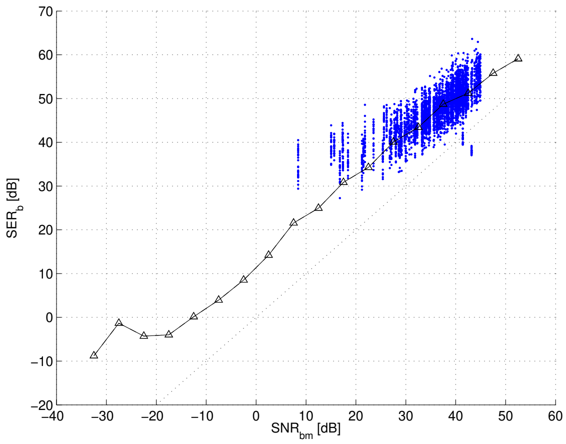


Fig. 3. Median bin-averaged SER (25) as a function of the minimal SNR within the bin, for 2-D quadratically interpolated GCG filter estimates (triangles), for a Jakes flat fading channel at 100 km/h. Kalman estimation gives the same performance. The cloud of points illustrates the distribution of the worst SNR (lowest channel power) within the bin $\text{SNR}_{mb}$ and the corresponding $\text{SER}_b$, when the average SNR is 40 dB. The dotted line indicates $\text{SNR}_{mb} = \text{SER}_b$.

Fig. 4 shows some preliminary results from performing long-range prediction in the frequency domain, using (22). The NMSE (23) is shown at SNR 20 dB as a function of the prediction horizon, scaled in carrier wavelengths. The results are compared to that of using the average power as predictor (upper solid, NMSE=0.5). It is also compared to the theoretical performance of perfectly adjusted 16-tap FIR predictors in the time domain, that utilize noise reduced regressors, from Fig. 2 in [13]. Frequency-domain Kalman predictors with $p = 4$ (dashed) and $p = 8$ (dash-dotted) outputs give NMSE's that correspond to the time-domain FIR results for short prediction horizons. They do however have a higher NMSE for longer horizons.

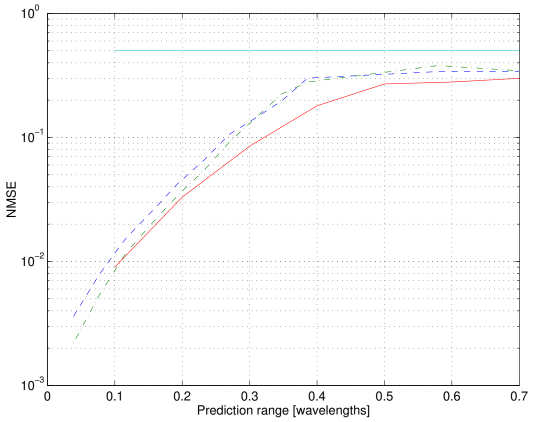


Fig. 4. Prediction NMSE as function of the prediction horizon at SNR 20 dB on the Jakes flat fading channel for Kalman predictors that use $p = 4$ (dashed) and $p = 8$ (dash-dotted) outputs. Compare to average predictor $\hat{p}_{n,t} = \sigma_h^2$ (upper solid) and an unbiased quadratic prediction in the time domain, based on a 16 tap sub-sampled FIR predictor from [13] (lower solid).

## IX. TEST ON A MEASURED CHANNEL

We finally illustrate the noise reduction properties on a 5 MHz channel measured in suburban Stockholm at 1880 MHz. This particular channel has delay spread 0.28 $\mu$s and a 3 dB coherence bandwidth of 6.4 MHz, see Fig 5. The mobile travels at 92 km/h, corresponding to a maximal Doppler frequency of 161 Hz. See also pp. 239-241 in [14].

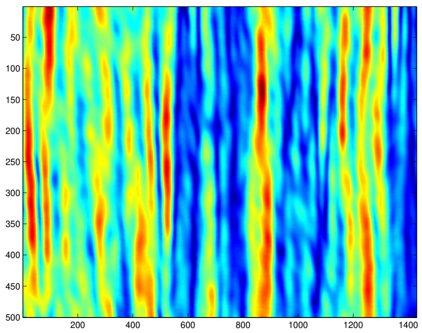


Fig. 5. Time-frequency plot of channel power. Vertical scale is subcarrier number and horizontal scale is symbol number.

The channel is estimated as described in [14] and this estimate is used as the true channel.[3] One estimator is then used for each bin width of 20 subcarriers. Thus, $p = 4$. Both the Kalman and the GCG algorithms are based on autoregressive models of order 4 that are adjusted to the Jakes fading spectrum. The channel statistics deviates significantly from the Jakes Rayleigh fading statistics, so there is a model mismatch. Accurate estimates of the noise and channel covariances are used. The resulting SER is shown in Fig. 6 as a function of the SNR. In contrast to the Jakes channel of Fig. 2, the GCG algorithm here has a higher estimation error (lower SER) than the Kalman algorithm. The two algorithms are affected in a similar way by regressor estimation errors at low SNR's.

[3]We thank Ericsson Research for providing measurements and Torbjörn Ekman for providing the estimated channel.

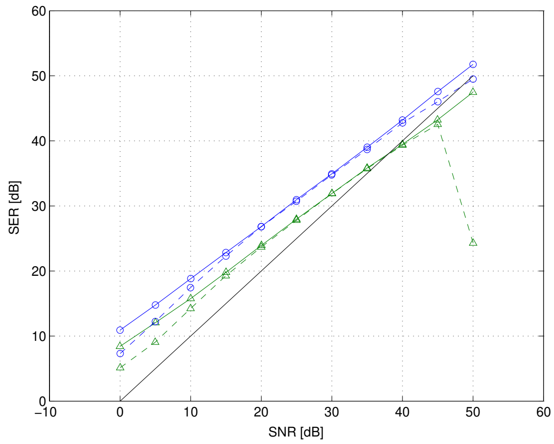


Fig. 6. Channel signal to estimation error ratio (SER) as a function of the SNR for the channel shown in Fig. 5, that is estimated from channel sounding data. Kalman (rings) and GCG (triangle) filter estimates $\hat{h}_{n,t|t}$ are obtained when using correct regressors (solid) and when using estimated downlink control symbols (dashed). The solid line SER=SNR is added for comparison. (The point at SNR=50 dB, SER=24 dB is due to numerical misbehavior.)

## REFERENCES

[1] Online: www.signal.uu.se/Research/PCCwirelessIP.html.
[2] M. Sternad, T. Ottosson, A. Ahlén and A. Svensson, "Attaining both coverage and high spectral efficiency with adaptive OFDM downlinks," *VTC 2003-Fall*, Orlando, Fla, Oct. 2003.
[3] W. Wang, T. Ottosson, M.Sternad, A. Ahlén and A. Svensson, "Impact of multiuser diversity and channel variability on adaptive OFDM" *VTC 2003-Fall*, Orlando, Fla, Oct. 2003.
[4] M. Sternad, L. Lindbom and A. Ahlén, "Wiener design of adaptation algorithms with time-invariant gains," *IEEE Trans. on Signal Proc.*, vol. 50, Aug. 2002, pp. 1895-1907.
[5] P. Hoeher, S. Kaiser and P. Robertson, "Two-dimensional pilot-symbol-aided channel estimation by Wiener filtering," *IEEE International Conference on Acoustics, Speech and Signal Processing*, 1997, pp. 1845-1848.
[6] Y. Li, L.J.Cimini and N. Sollenberger, "Robust channel estimation for OFDM systems with rapid dispersive fading channels," *IEEE Trans. on Communications*, vol. 46, pp. 902-915, 1998.
[7] O. Edfors, M. Sandell, J-J van de Beek, S.K. Wilson and P.O. Börjesson, "OFDM channel estimation by singular value decomposition," *IEEE Trans. on Communications*, vol. 46, pp. 931-939, 1998.
[8] B.D.O. Anderson and J.B. Moore, *Optimal Filtering*. Prentice-Hall, Englewood Cliffs, NJ, 1979.
[9] T. Kailath, A.H. Sayed and B. Hassibi, *Linear Estimation* Prentice-Hall, Upper Saddle River, NJ, 2000.
[10] L. Lindbom, M. Sternad and A. Ahlén, "Tracking of time-varying mobile radio channels. Part I: The Wiener LMS algorithm". *IEEE Trans. on Commun*, vol 49, pp. 2207-2217, Dec. 2001.
[11] L. Lindbom, A. Ahlén, M. Sternad and M. Falkenström, "Tracking of time-varying mobile radio channels. Part II: A case study". *IEEE Trans. on Commun*, vol 50, pp. 156-167, Jan. 2002.
[12] M-X Chang and Y.T. Su, "Model-based channel estimation for OFDM signals in Rayleigh fading," *IEEE Trans. on Communications*, vol. 50, pp. 540-544, 1998.
[13] T. Ekman, M. Sternad and A. Ahlén, "Unbiased power prediction on broadband channels," *IEEE Vehicular Technology Conference*, Fall 2002, Vancouver, Canada, Sept. 24-28 2002.
[14] T. Ekman *Prediction of Mobile Radio Channels. Modeling and Design* PhD Thesis, Signals and Systems, Uppsala University, Sweden, 2002. Online: www.signal.uu.se/Publications/abstracts/a023.html